JOURNAL OF SOLID STATE CHEMISTRY **127,** 31–39 (1996)
ARTICLE NO. 0353

Influence of Stacking Faults and Temperature on the Structure of $Y_2Ba_4Cu_7O_{15}$, Investigated by High-Resolution Neutron Diffraction and Electron Microscopy

P. Berastegui,*[,1] P. Fischer,† I. Bryntse,‡ L.-G. Johansson,* and A. W. Hewat§

*Department of Inorganic Chemistry GU, CTH, S-41296 Göteborg, Sweden; †Laboratory for Neutron Scattering, ETH Zurich & Paul Scherrer Institute, CH-5232 Villingen PSI, Switzerland; ‡Department of Inorganic Chemistry, Arrhenius Laboratory, Stockholm University, S-10691 Stockholm, Sweden; and §Institut Laue-Langevin, BP 156, F-38042 Grenoble, France

Received April 1, 1996; in revised form July 23, 1996; accepted August 1, 1996

The temperature dependence of the structure of the high-T_c superconductor $Y_2Ba_4Cu_7O_{15-\delta}$ (Y-247) has been studied by high-resolution neutron powder diffraction. This structure can be described as alternating single CuO chain (123) and double CuO chain (124) blocks. Two fully oxidized polycrystalline Y-247 samples with $T_{c,onset}$ = 94.8 and 89.3 K, prepared by a sol–gel technique at 1 atm oxygen pressure, were investigated in the temperature range from 5 to 100 K, and the structural changes were determined by Rietveld analysis. The oxygen content was found to be equal in both samples but the unit cell parameters and interatomic bond distances differed significantly. The structural changes with temperature in the compound with $T_{c,onset} \approx 95$ K showed that the displacements of the apical oxygen in the 123 and 124 blocks are different. In agreement with the decreased coherence length along the *c* axis detected by neutron diffraction, electron diffraction studies showed considerable streaking in the sample with T_c = 89 K whereas the sample with T_c = 95 K was more ordered. High-resolution electron microscopy studies indicated that the reason for streaking are stacking faults in the –123–124–123–124– sequence that build up the structure.

1. INTRODUCTION

$Y_2Ba_4Cu_7O_{15}$ (Y-247) is a high-T_c superconductor belonging to the $Y_2Ba_4Cu_{6+n}O_{14+n-\delta}$ series. In $YBa_2Cu_3O_{7-\delta}$ (Y-123, $n = 0$), oxygen can be removed from the single CuO chains to obtain linearly coordinated Cu, thereby reducing the hole content at the CuO_2 planes and suppressing superconductivity. $YBa_2Cu_4O_8$ (Y-124, $n = 2$) exhibits a double chain, where oxygen is more strongly coordinated. The oxygen content is thus constant up to about 850°C in an oxygen atmosphere, at which temperature the compound decomposes to Y-123 and CuO. The Y-247 ($n = 1$) structure can be considered as an intergrowth of alternating 123 and 124 blocks stacked along the *c* axis; see Fig. 1. In the text, the notations Y-123 and 123 block will be used to designate the pure phase and the corresponding block in the Y-247 phase, respectively. Oxygen can be removed from the 123 block as in Y-123, while the structure retains its orthorhombicity due to the stability of the double chain in the 124 block.

It is known that the oxygen content in $Y_2Ba_4Cu_7O_{15-\delta}$ can be varied from $\delta = 0.9$ to $\delta = -0.3$, thereby increasing the superconducting transition from 30 to 95 K (1). $T_{c,onset}$ values reported by different groups, for both a number of fully oxidized Ln-247 samples and Y-247 samples, vary from the highest reported value of 95 K to values close to 40 K (1–15). This spread, as well as the width of the superconducting transition, is suggested to be due, not mainly to a variation in oxygen content but to the presence of microstructural defects in the samples. In the work of Guo *et al.* (16), the microstructure of two Y-247 samples with different T_c was studied. The sample with highest T_c, 95 K, was observed to show only dislocations while the sample with lower T_c displayed a large number of periodically ordered stacking faults. It was suggested that the stacking faults decrease T_c, while dislocations do not affect T_c.

As previously mentioned, the $Y_2Ba_4Cu_7O_{15-\delta}$ phase retains its orthorhombicity at high temperature due to the presence of the double chain in the 124 block, and does not undergo a transition to tetragonal symmetry as $Y_1Ba_2Cu_3O_{7-\delta}$. Thermogravimetry measurements have shown that oxygen is gradually depleted as Y-247 is heated (17). Thus, the oxygen content can be controlled by, e.g., slow cooling from high temperature and annealing in oxygen. However, the formation of stacking faults is more difficult to control, the stability range for the material which is free from stacking faults being very small. Moreover, only a small number of reports describe the synthesis of high quality polycrystalline samples with $T_c \approx 95$ K (6, 18).

[1] To whom correspondence should be addressed.

0022-4596/96 $18.00

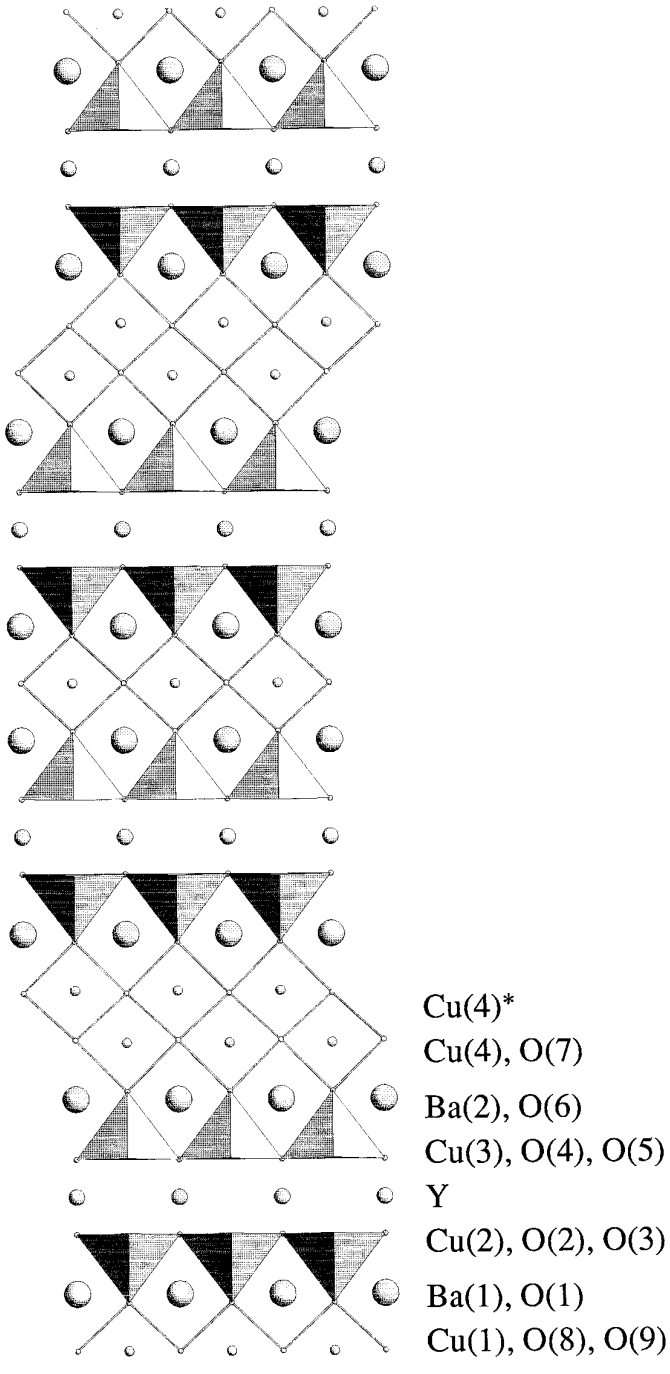

FIG. 1. Projection along [100] of the crystal structure of $Y_2Ba_4Cu_7O_{15}$ illustrating the nomenclature used and the sequence of single chain and double chain blocks.

This indicates the difficulty in preparing this phase, and its sensitivity to synthesis conditions.

In this work, we report the first high-resolution ($\Delta d/d = 2 \times 10^{-3}$, d = lattice spacing) neutron diffraction results on the structural changes that occur with temperature for a Y-247 sample with maximum T_c = 95 K. The structural differences and microstructure in two Y-247 samples with different T_c values are discussed.

2. EXPERIMENTAL

Polycrystalline samples were synthesized from precursors prepared by a polymerized complex method (19). The precursors were sintered at around 865°C at 1 atm oxygen pressure for 2 weeks, with intermediate grinding and pelletizing. In order to obtain fully oxygenated samples, annealing in oxygen at 400°C was carried out for 4 days. X-ray diffractograms for both samples taken with a Siemens D-5000 powder diffractometer using CuKα radiation are shown in Fig. 2. No impurities, such as CuO or $BaCuO_2$, could be detected in the samples, but differences in both peak intensity and sharpness indicate the presence of microstructural defects in the sample with lower T_c. It was found that the quality of the precursor or green body and the sintering temperature were the determining factors in the preparation of samples with the highest T_c values. Thus, the irreversible formation of microstructural defects may be observed at early stages in the sintering procedure. In order to prepare the 95 K Y-247 sample the temperature had to be controlled to within 865 ± 5°C.

The superconducting transition temperature was measured in terms of the complex ac susceptibility. The real and imaginary parts of the magnetic susceptibility versus temperature for a frequency of 132 Hz and amplitude 100 mOe are shown in Fig. 3. The single peak appearing on the χ'' curve implies that these samples contain only one superconducting phase, although the superconductivity transition is broader, $\Delta T \approx 6$ K, for the sample with $T_{c,\,onset}$ = 89.3 K. The observed $T_{c,\,onset}$ for the $Y_2Ba_4Cu_7O_{15-\delta}$ sample, 94.8 K with ΔT (10–90%) = 3 K, indicates the high quality of this sample.

High-resolution neutron diffraction measurements were performed on the D2B instrument at the ILL, Grenoble, high-flux reactor in the high intensity mode with an angular stepwidth of 0.05° in 2θ, and wavelength of λ = 1.5943 Å. Each diffraction pattern was measured eight times at each temperature. The samples were enclosed in a He filled vanadium container and cooling was performed in a ILL ''orange'' He-flow cryostat. Rietveld analyses were carried out with the program FULLPROF (20). Figure 4 shows the profile fits obtained for both samples which are considerably improved compared to the previous Y-247 neutron diffraction investigation of a polycrystalline sample prepared by a high oxygen pressure technique (21).

The cation content was analyzed for the two samples by energy-dispersive spectrometry (EDS) in a scanning electron microscope (JEOL 820), using the L-lines for Y and Ba and the K-lines for Cu. Selected-area electron diffraction patterns of the same samples were obtained in

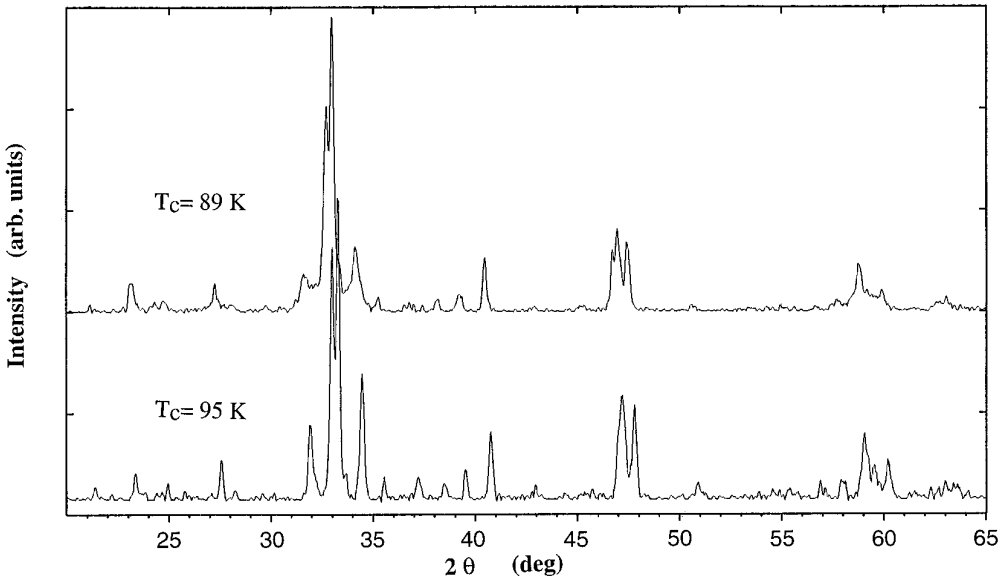

FIG. 2. X-ray diffractogram patterns (Cu$K\alpha$) of the two $Y_2Ba_4Cu_7O_{15}$ samples studied in this work, with T_c = 89 K (above) and T_c = 95 K (below). The sample with T_c = 89 K exhibits peak broadening in comparison with the sample with T_c = 95 K.

transmission electron microscopes (JEOL 2000FX, 200CX, and 3010). The first microscope was also equipped with an EDS detector (LINK QX200) in the high angle (70°) position, and the two latter were used for high resolution studies. The specimens were prepared by crushing the powder in butanol and then a droplet was put on a metal grid covered with a holey carbon film.

3. RESULTS AND DISCUSSION

The dependence of the structural parameters on temperature for two $Y_2Ba_4Cu_7O_{15-\delta}$ samples with different T_c was studied at 5, 45, 80 and 100 K. Rietveld analysis of the neutron diffraction data included the refinement of an overall temperature factor for each atom type and a parameter for anisotropic particle size broadening. The latter was found to improve the refined model for the sample with lower T_c, decreasing the χ^2 value in the refinement. It should be mentioned at this point that powder neutron diffraction gives averaged and quantitative statistical information on the crystal structure of the sample under study. Microstructural defects can thus be observed and described by models, that are characterized by the shapes and widths of the Bragg reflections through a number of size and strain

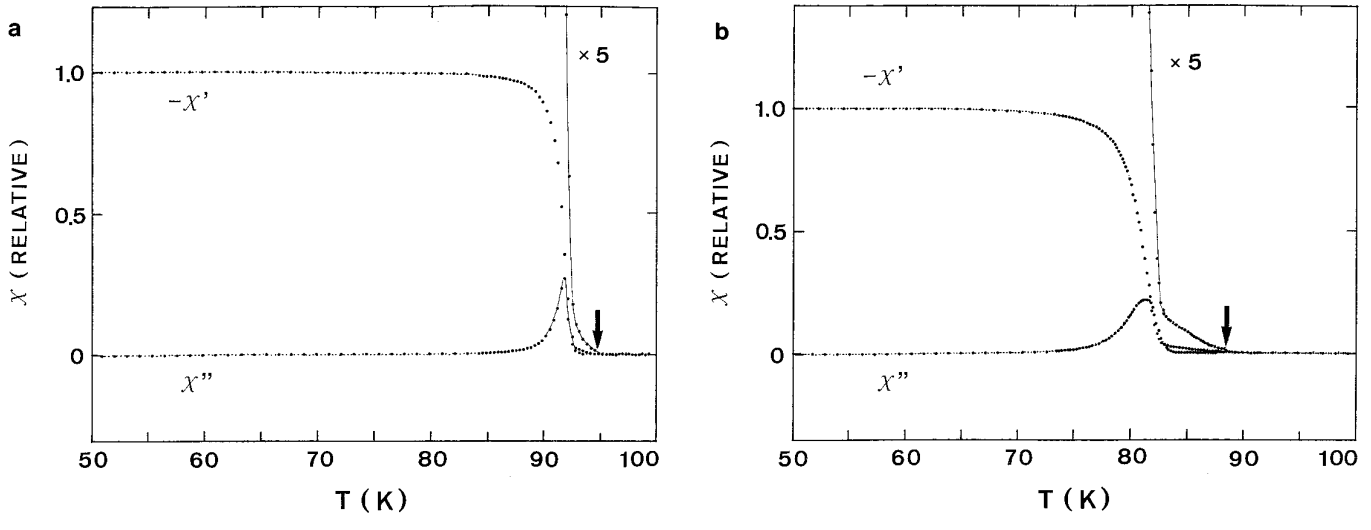

FIG. 3. Real and imaginary parts of the magnetic susceptibility, χ, vs temperature for the two $Y_2Ba_4Cu_7O_{15}$ samples. The amplitude of the applied field is 100 mOe. The onset temperatures are 94.8 and 89.3 K (indicated by the arrows).

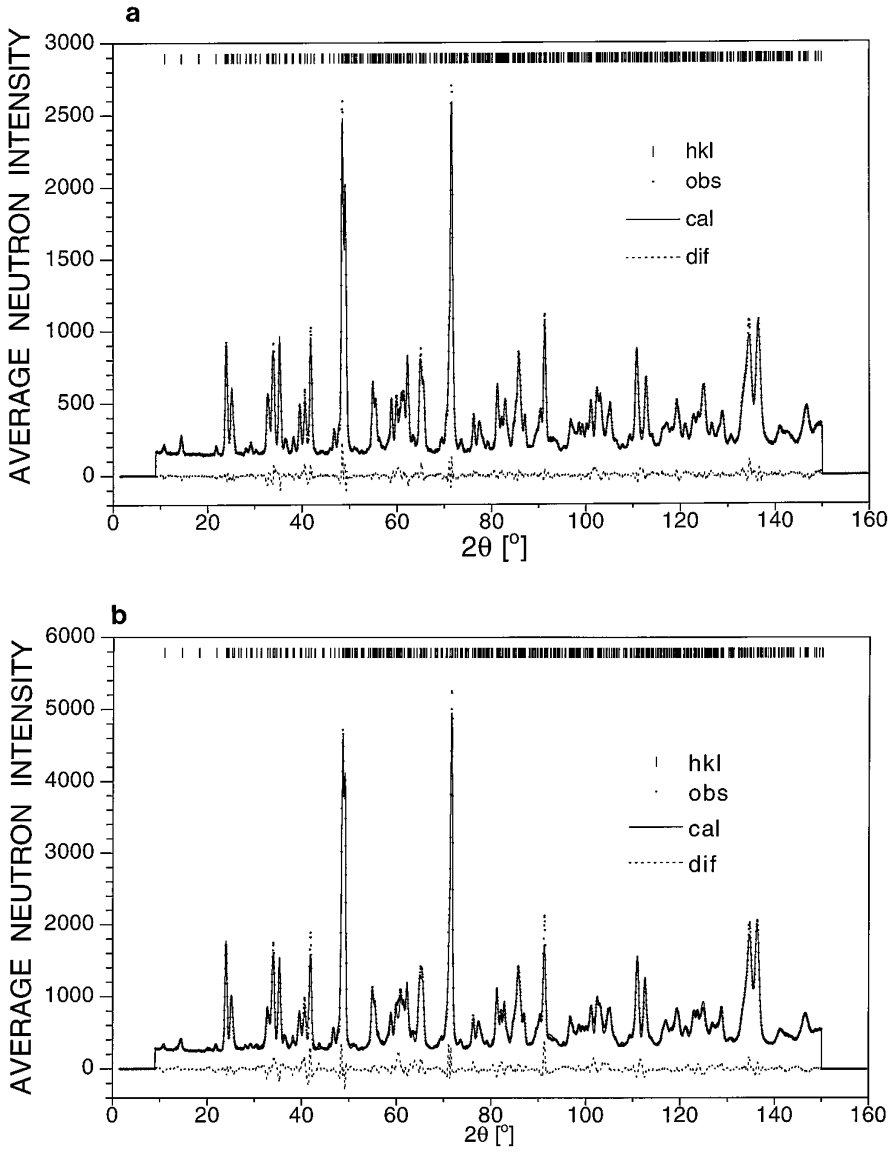

FIG. 4. Observed, calculated, and difference neutron diffraction patterns for $Y_2Ba_4Cu_7O_{15}$ at 5 K with (a) $T_c = 95$ K and (b) $T_c = 89$ K. The neutron wavelength was $\lambda = 1.5943$ Å. The peak positions are marked on top.

parameters. We obtained the best fits with Thompson–Cox–Hastings pseudo-Voigt peak shape (20) with a *Y* parameter. Platelet-like coherent domains were assumed for the anisotropic part of line broadening. The size model was described by size $\times \cos(\phi)$, where ϕ is the angle between the scattering vector and the normal to the platelets which was taken as [0,0,1]. This approximation yielded the size parameters 0.083(7) and 0.294(16) for the Y-247 samples with $T_c = 95$ and 89 K, respectively (5 K data). This implies a considerably smaller domain size or correlation length (of the order of 200 Å) along the *c* direction in the sample with lower T_c which confirms the increased number of stacking faults observed by high-resolution electron microscopy studies in this specimen. As the instrumental parameters were not precisely known at the time of the neutron investigations, a more quantitative domain size determination is difficult from the present neutron data.

Table 1 shows the calculated atomic parameters and reliability factors for both samples. The oxygen occupancies at the single chain were refined at the positions O(8) and O(9), i.e., parallel and perpendicular to the *b* axis, respectively. It was found that the sum of their values added to about 100% single chain oxidation in both samples and at all temperatures. Therefore, the sum of site occupancies was subsequently constrained to 1.0 in the final refinement. All other occupancies were fixed at their nominal

TABLE 1
Structural Parameters for $Y_2Ba_4Cu_7O_{15}$ Samples with T_c = 95 K (bold) and T_c = 89 K (plain): Space Group *Ammm* (No. 65); Z = 4

T:			**5 K**	**45 K**	**80 K**	**100 K**	5 K	45 K	80 K	100 K
a	(Å)		**3.8293(1)**	**3.8294(1)**	**3.8297(1)**	**3.8300(1)**	3.8329(1)	3.8330(1)	3.8333(1)	3.8338(1)
b	(Å)		**3.8718(1)**	**3.8719(1)**	**3.8719(1)**	**3.8720(1)**	3.8690(1)	3.8690(1)	3.8690(1)	3.8693(1)
c	(Å)		**50.465(1)**	**50.467(1)**	**50.482(1)**	**50.492(1)**	50.462(3)	50.466(3)	50.480(3)	50.491(3)
V	(Å^3)		**748.21(4)**	**748.27(4)**	**748.57(4)**	**748.78(4)**	748.31(5)	748.39(5)	748.67(5)	748.99(5)
Y	4*j*	*z*	**0.11532(7)**	**0.11528(7)**	**0.11527(7)**	**0.11529(7)**	0.1155(1)	0.1154(1)	0.1154(1)	0.1154(1)
		B (Å^2)	**0.40(4)**	**0.42(4)**	**0.47(4)**	**0.48(4)**	0.42(6)	0.43(6)	0.49(6)	0.55(6)
Ba(1)	4*j*	*z*	**0.04211(8)**	**0.04219(7)**	**0.04216(8)**	**0.04218(8)**	0.0427(1)	0.0427(1)	0.0427(1)	0.0427(1)
		B (Å^2)	**0**	**0**	**0**	**0**	0	0	0	0
Ba(2)	4*j*	*z*	**0.18744(8)**	**0.18746(8)**	**0.18747(8)**	**0.18745(8)**	0.1869(1)	0.1868(1)	0.1870(1)	0.1870(1)
		B (Å^2)	**0**	**0**	**0**	**0**	0	0	0	0
Cu(1)	2*a*	*B* (Å^2)	**0.32(2)**	**0.34(2)**	**0.36(2)**	**0.38(2)**	0.34(3)	0.36(3)	0.37(3)	0.40(3)
Cu(2)	4*i*	*z*	**0.08160(5)**	**0.08168(5)**	**0.08169(5)**	**0.08167(5)**	0.08169(9)	0.08171(9)	0.08171(9)	0.08179(9)
		B (Å^2)	**0.32(2)**	**0.34(2)**	**0.36(2)**	**0.38(2)**	0.34(3)	0.36(3)	0.37(3)	0.40(3)
Cu(3)	4*i*	*z*	**0.14858(5)**	**0.14859(5)**	**0.14858(6)**	**0.14861(6)**	0.1485(1)	0.1485(1)	0.1485(1)	0.1486(1)
		B (Å^2)	**0.32(2)**	**0.34(2)**	**0.36(2)**	**0.38(2)**	0.34(3)	0.36(3)	0.37(3)	0.40(3)
Cu(4)	4*i*	*z*	**0.23034(4)**	**0.23034(4)**	**0.23036(4)**	**0.23039(4)**	0.23037(8)	0.23035(8)	0.23039(8)	0.23036(8)
		B (Å^2)	**0.32(2)**	**0.34(2)**	**0.36(2)**	**0.38(2)**	0.34(3)	0.36(3)	0.37(3)	0.40(3)
O(1)	4*i*	*z*	**0.03640(9)**	**0.03646(9)**	**0.03634(9)**	**0.0363(1)**	0.0368(2)	0.0368(2)	0.0368(2)	0.0366(1)
		B (Å^2)	**0.46(2)**	**0.48(2)**	**0.49(2)**	**0.54(2)**	0.43(2)	0.45(2)	0.48(2)	0.49(3)
O(2)	4*j*	*z*	**0.08690(8)**	**0.08693(8)**	**0.08705(9)**	**0.08699(9)**	0.0866(2)	0.0865(2)	0.0866(2)	0.0866(1)
		B (Å^2)	**0.46(2)**	**0.48(2)**	**0.49(2)**	**0.54(2)**	0.43(2)	0.45(2)	0.48(2)	0.49(3)
O(3)	4*i*	*z*	**0.08679(7)**	**0.08679(7)**	**0.08679(7)**	**0.08684(7)**	0.0861(1)	0.0861(1)	0.0861(1)	0.0861(1)
		B (Å^2)	**0.46(2)**	**0.48(2)**	**0.49(2)**	**0.54(2)**	0.43(2)	0.45(2)	0.48(2)	0.49(3)
O(4)	4*j*	*z*	**0.14386(8)**	**0.14383(8)**	**0.14388(8)**	**0.14385(8)**	0.1445(1)	0.1444(1)	0.1446(1)	0.1447(1)
		B (Å^2)	**0.46(2)**	**0.48(2)**	**0.49(2)**	**0.54(2)**	0.43(2)	0.45(2)	0.48(2)	0.49(3)
O(5)	4*i*	*z*	**0.14349(7)**	**0.14344(7)**	**0.14345(8)**	**0.14346(8)**	0.1431(1)	9.1432(1)	0.1431(1)	0.1431(1)
		B (Å^2)	**0.46(2)**	**0.48(2)**	**0.49(2)**	**0.54(2)**	0.43(2)	0.45(2)	0.48(2)	0.49(3)
O(6)	4*i*	*z*	**0.19371(8)**	**0.19367(8)**	**0.19368(8)**	**0.19366(8)**	0.1938(1)	0.1938(1)	0.1938(1)	0.1938(1)
		B (Å^2)	**0.36(2)**	**0.48(2)**	**0.49(2)**	**0.54(2)**	0.43(2)	0.45(2)	0.48(2)	0.49(3)
O(7)	4*i*	*z*	**0.23277(8)**	**0.23279(8)**	**0.23272(8)**	**0.23271(8)**	0.2328(1)	0.2328(1)	0.2328(1)	0.2329(1)
		B (Å^2)	**0.46(2)**	**0.48(2)**	**0.49(2)**	**0.54(2)**	0.43(2)	0.45(2)	0.48(2)	0.49(3)
O(8)	2*b*	*B* (Å^2)	**0.46(2)**	**0.48(2)**	**0.49(2)**	**0.54(2)**	0.43(2)	0.45(2)	0.48(2)	0.49(3)
		n	**0.76(1)**	**0.77(1)**	**0.76(1)**	**0.76(1)**	0.65(1)	0.65(1)	0.64(1)	0.64(1)
O(9)	2*d*	*B* (Å^2)	**0.46(2)**	**0.48(2)**	**0.49(2)**	**0.54(2)**	0.43(2)	0.45(2)	0.48(2)	0.49(3)
		n	**0.24(1)**	**0.23(1)**	**0.24(1)**	**0.24(1)**	0.35(1)	0.35(1)	0.36(1)	0.36(1)
R_p	(%)		**3.70**	**3.64**	**3.70**	**3.72**	5.52	5.52	5.46	5.46
R_{wp}	(%)		**4.79**	**4.75**	**4.81**	**4.82**	7.40	7.40	7.36	7.38
R_B	(%)		**3.26**	**3.23**	**3.36**	**3.43**	5.06	5.10	5.10	4.89

values. As can be seen from the table, the O(8) site occupancy is 76% in the sample with T_c = 95 K, while it decreases to 64% in the sample with T_c = 89 K. In the work of Hewat *et al.* (21), occupancies of 71% for O(8) and 32% for O(9) are obtained for a sample with T = 68 K. This implies that the different T_c value of the two samples is not caused by different oxygen contents or by different site occupancies in the CuO single chain region. Instead we consider that the stacking faults are the cause of the lower T_c in the 89 K sample, as has also been shown by Guo *et al.* (16).

Although the observed trends in atomic parameters and bond distances for the two samples are similar, some significant differences were found. For example, the bond distances in the chain region of the 124 block, were found to be more difficult to describe consistently in the refinements for the sample with lower T_c. This is indicative of the stacking disorder in this sample. Also, $Cu_{in\text{-}plane}$–O_{apical} (abbreviated Cu_{pl}–O_{ap}) and Y–O_{pl} distances are found to be equal in the two blocks in the sample with higher T_c, while different values are exhibited in the sample with lower T_c. In the following discussion, the temperature dependence of the structure for the 95 K sample will be treated, and then the structural parameters and observations from a microstructural investigation of the two samples will be compared.

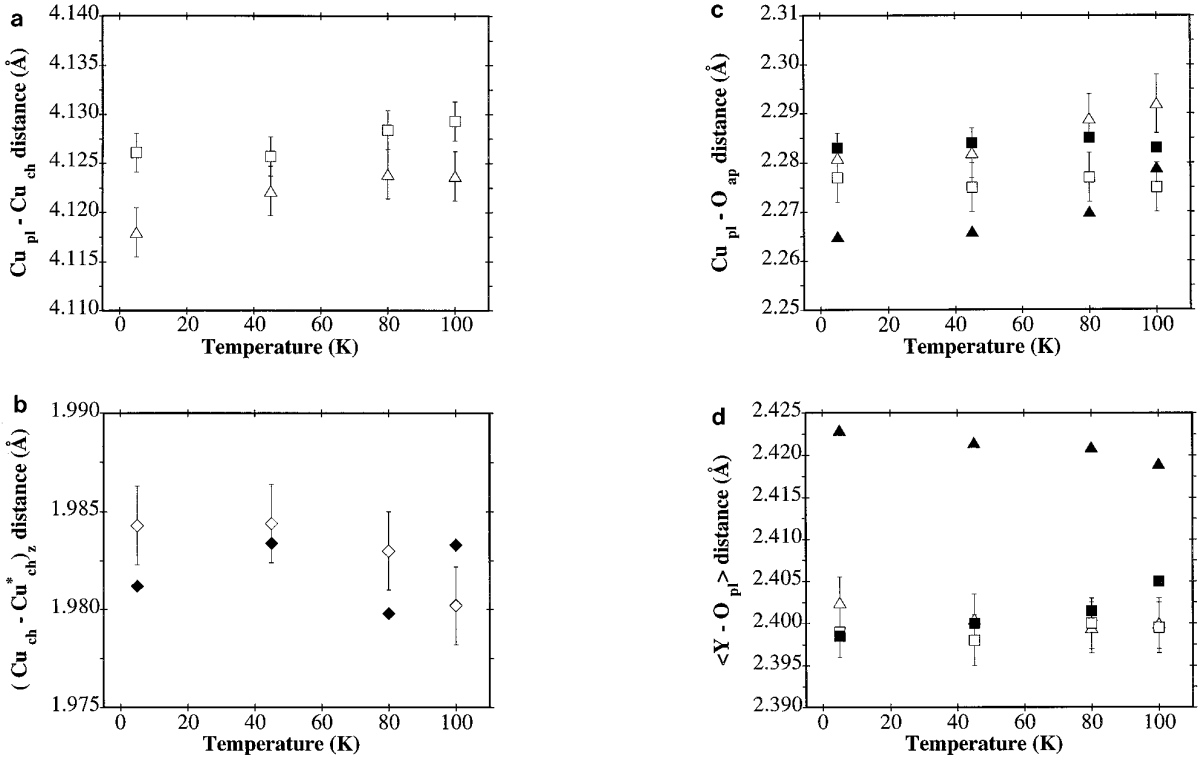

FIG. 5. Temperature dependence of some relevant bond distances in two $Y_2Ba_4Cu_7O_{15}$ samples with T_c = 95 K (open symbols) and T_c = 89 K (solid symbols) (123-block (△); 124-block (□)). Some error bars have been omitted for clarity.

3.1. Temperature Dependence

The temperature dependence of the structure of $Y_2Ba_4Cu_7O_{15-\delta}$ has been studied previously by Hewat *et al.* (21) using a sample with T_c = 68 K prepared by a high oxygen pressure technique (22). The authors report an anisotropic thermal expansion, which is due to the more rigid *b* axis, and significant changes in the coordination of the apical oxygen in the 123 and 124 blocks. Although the orthorhombicity is greater and the *c* axis longer in the present investigation compared to the work of Hewat *et al.,* we observe similar changes with temperature, the *c* axis increasing rapidly.

Most interatomic distances did not change significantly with temperature, except for the bonds between copper and the apical oxygen. Figure 5 shows some relevant interatomic distances in the chain region. A small increase of the Cu_{plane}–Cu_{chain} (abbreviated Cu_{pl}–Cu_{ch}) distance with temperature can be observed in both blocks. This increase is compensated by a decrease of the distance between the Cu atoms in the double chain along the *c* axis, Cu_{ch}–Cu_{ch}*, of approximately the same magnitude. Considering the bonds between copper and the apical oxygen, an increase can be observed with temperature in the Cu_{pl}–O_{ap} distance in the 123 block, while the corresponding distance remains constant in the 124 block. The Cu_{pl}–O_{ap} bond in Y-123 is known to be elongated as holes are removed from the CuO_2 planes (23). The changes in bond lengths observed may thus be interpreted in terms of a transfer of positive charge from the CuO_2 planes to the single chain in the 123 block. The 124 block responds to the temperature increase by decreasing the Cu_{ch}–Cu_{ch}* distance in the double chain, while other distances remain constant. Thus, as previously suggested (21), the 123 block responds to charge transfer, while the 124 block merely relieves the structural strain through the larger double chain volume.

3.2. The Effects of Structural Disorder

It has been shown (24, 25), that the cell parameters of the Y-247 phase behave as in Y-123 with oxygen depletion, i.e., the orthorhombicity decreases and the *c* axis increases. The difference in *c* axis between the two samples studied is small and within standard deviations, with a mean value of 50.464 Å at 5 K. It is then reasonable to assume that the oxygen content is the same in both samples, which is supported by the refined oxygen occupancies. We therefore conclude that the difference in the orthorhombicity factor between the 95 and 89 K samples is caused by the presence of microstructural defects; see Fig. 6. Moreover, it is proposed that T_c in fully oxygenated Y-247 is directly related to the concentration of stacking faults and that this is reflected in a smaller orthorhombicity. The presence of microstructural defects also results in irregularities in the

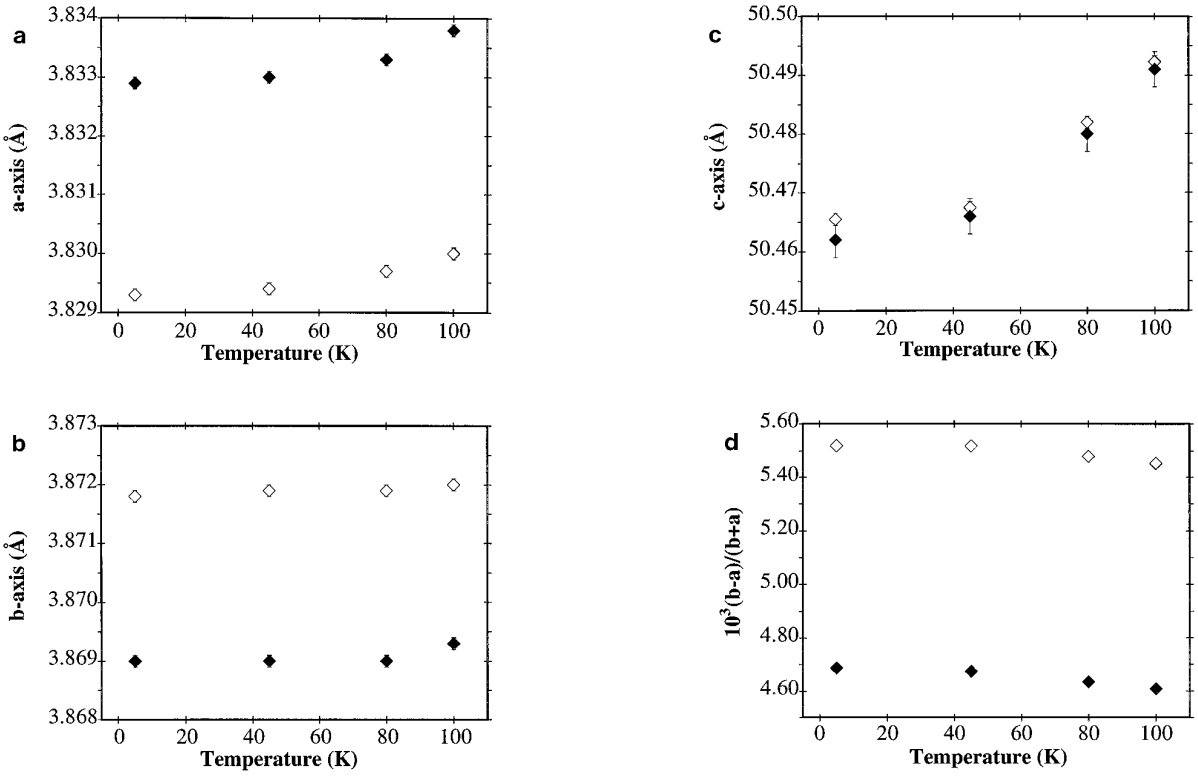

FIG. 6. Temperature dependence of cell parameters and orthorhombicity expressed as 10^3 (b − a)/(b + a), in the two $Y_2Ba_4Cu_7O_{15}$ samples with T_c = 95 K (open symbols) and T_c = 89 K (solid symbols).

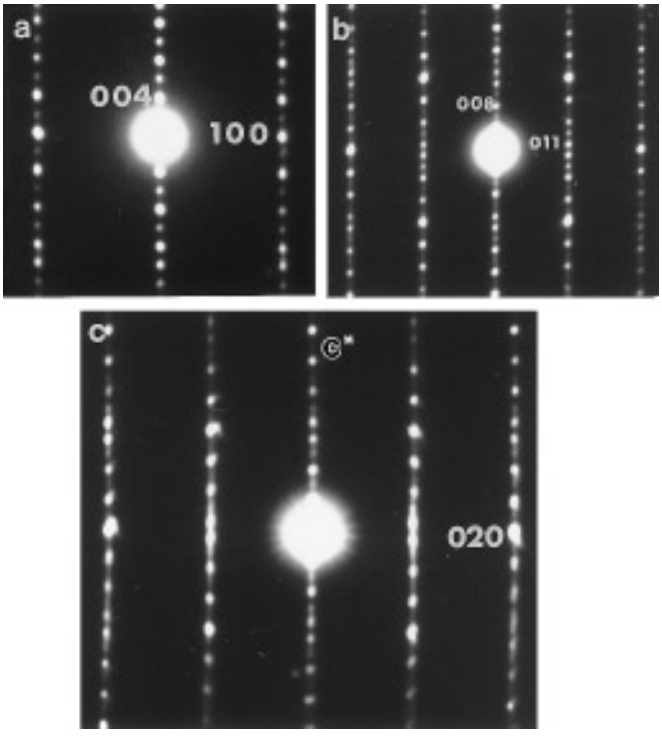

FIG. 7. A well ordered selected-area electron diffraction pattern in the [010] zone of $Y_2Ba_4Cu_7O_{15}$ with a T_c of 95 K is shown in (a). (b) and (c) show streaked patterns along [100] of Y-247 crystallites from the sample with a T_c of 89 K.

Cu_{ch}–Cu_{ch}* distance, although the overall trends are the same as those observed for the sample with T_c = 95 K. In Fig. 5, the distances between Y and the plane oxygen ions in each block are presented. As can be seen, for the sample with T_c = 95 K, the mean Y–O_{pl} distance to the two blocks is the same for the temperature range studied. As discussed in (16), the extraction of a CuO layer is an intrinsic stacking fault in Y-247, and Fig. 5 (Cu_{ch}–Cu_{ch}* distance) shows how the refined bond distances in the double chain are affected by the presence of stacking faults, showing irregular trends. The similarity in trends in bond distances with temperature is illustrated by the Cu_{pl}–O_{ap} distances in Fig. 5, i.e., the Cu_{pl}–O_{ap} distance increases in the 123 block and remains constant in the 124 block. However, it is apparent that the interpretation of the refined data can be misleading when the sample contains microstructural defects.

3.3. Microstructural Studies by Electron Microscopy

EDS analyses made in the transmission and scanning microscopes indicated that the samples with superconducting transitions at 89 and 95 K had the desired composition. It was not possible to detect any significant deviation from the nominal stoichiometry. This is an additional evidence that the sol–gel synthesis worked well.

Selected-area electron diffraction photographs were also obtained (Fig. 7a–7c). The dimensions and symmetries of

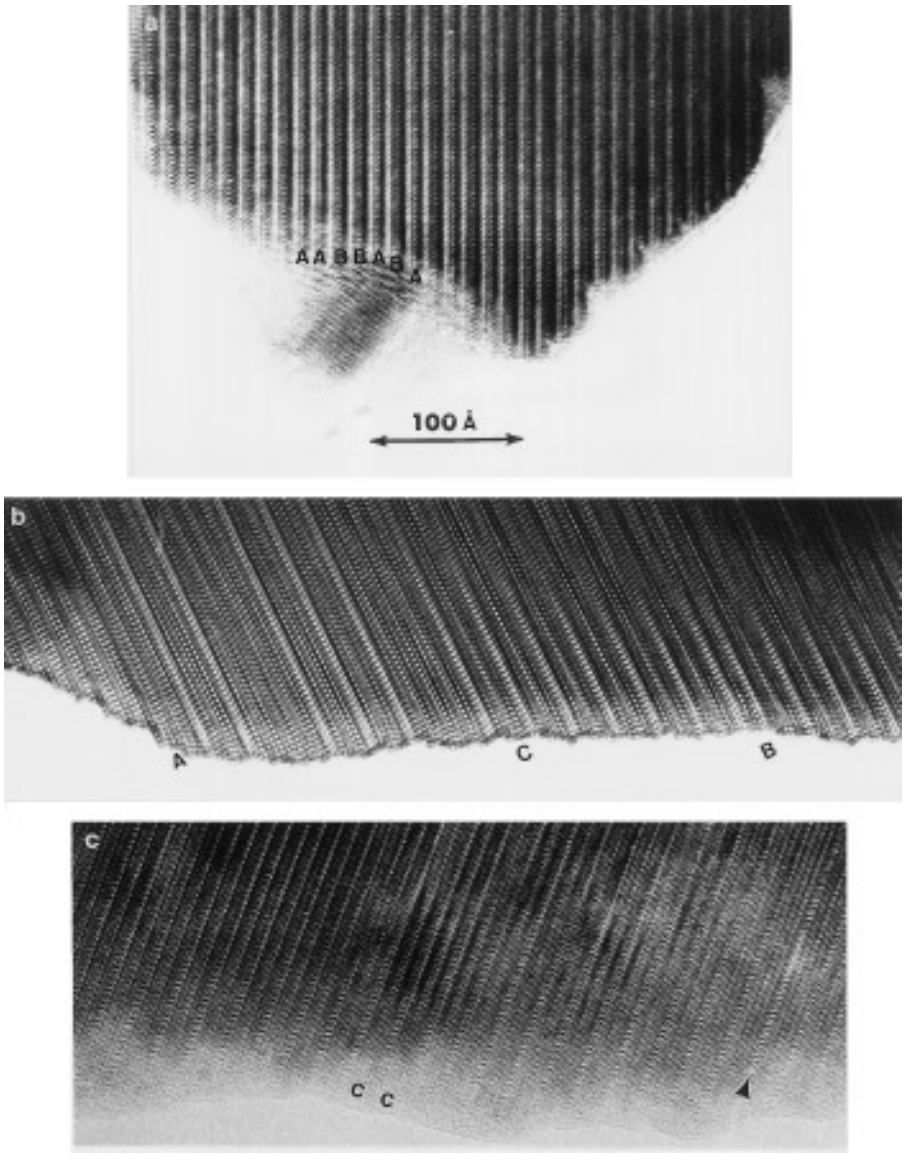

FIG. 8. High-resolution electron micrographs of the *ac* plane of $Y_2Ba_4Cu_7O_{15}$. (a) A relatively thick particle from the sample with T_c= 89 K, b) a slightly tilted crystallite from the 95 K sample (with the same magnification as in (a)), and (c) a more well-ordered area, where an arrow indicates a triple CuO block. Structural blocks of 123, 124, and 247 (–123–124–) are marked in the photographs with letters A, B, and C, respectively.

all the main reflections agreed with an *A*-centered unit cell having a *c* axis of approximately 50 Å. Figure 7a shows a relatively well ordered diffraction pattern typical for the compound with the highest T_c. However, almost all patterns taken from the sample with lower T_c were streaked along *c** (Figs. 7b and 7c). The streaking indicates that stacking faults, such as intergrowths, occur in the structure. Since the unit cell is *A* centered, a diffraction pattern of the *a***c** plane must differ from that of the *b***c** plane. Twinning caused by a mixing of *a* and *b* will be clearly seen as two diffraction patterns superimposed upon each other, as was recently found in a study of 124 synthesized by a similar type of sol–gel technique (26). No crystallites with such twinned patterns were found in this limited study, however. This result seems to agree with the electron microscopy investigation of 247 by Guo *et al.* (16).

High resolution studies of both samples confirmed that stacking faults were frequent; see Fig. 8a (89 K sample) and Figs. 8b and 8c (95 K sample). In Fig. 8b, blocks having a length of approximately 25 Å, i.e., half the unit cell are common. The brighter rows in this image correspond to the double CuO layers of the 124 block. Other variants such as –124–123–123–124– or –123–124–124–123– were also found, as indicated in Figs. 8a, and 8b. Another type of fault, a triple CuO block, was occasionally found (Fig. 8c). Note that only the thinnest edges are studied by this

technique whereas electron diffraction normally is obtained from a larger area. It was not possible to discern a superlattice type of structure with a c axis of 400 Å, as was reported by Guo *et al.* (16).

The cation composition of these 247 powders agreed with the nominal stoichiometry, which suggests that the number of 123 and 124 blocks is equal. Therefore the samples probably have the same overall oxygen content as was obtained from the structural refinements.

4. CONCLUSION

The temperature dependence of the structure of a Y-247 sample with $T_c = 95$ K was for the first time investigated by means of high-resolution neutron diffraction. In contrast to high oxygen pressure synthesis, sol–gel techniques at 1 atm oxygen pressure as used here, permit the preparation of rather large Y-247 specimens with high T_c values for neutron diffraction experiments.

The oxygen content in Y-247 can be controlled by annealing at different partial pressures of oxygen, while the preparation of defect ''free'' Y-247 samples requires a very precise control of the sintering temperature at the chosen pressure. Precursor quality also seems to play an important role in this respect. The different T_c values reported in the literature for Y-247 samples suggest that reactants, temperature, and pressure must be carefully chosen in order to obtain good quality Y-247 samples. We have also found that at atmospheric pressure, the formation of stacking faults is irreversible and that T_c in the fully oxygenated Y-247 phase is correlated to the amount of stacking faults present.

Although these microstructural defects also affect the oxygen distribution at the two possible sites in the single chain, they do not seem to affect the total oxygen content. The differences observed in the structural models for the two samples with different T_c values reveal the effect of the stacking faults, but the trends in bond distances are observed to be the same. The refined models at different temperatures for the sample with $T_c = 95$ K show a monotonic increase with temperature of the Cu_{pl}–O_{ap} bond distance in the 123 block from below T_c, that can be related to the transfer of positive charge from the planes to the chains. On the other hand, the corresponding distances in the 124 block do not show such changes and this block seems merely to respond to the strains caused by the change in temperature.

By high resolution electron microscopy stacking faults were observed to occur in both samples under study. The fact that the selected-area diffraction patterns showed streaking along c^* only for the low T_c sample indicates that the disorder is more pronounced.

ACKNOWLEDGMENTS

The authors acknowledge J. Rodriguez-Carvajal for a valuable discussion and also express their gratitude to Professor H. Mazaki and his research group for the susceptibility measurements. The Swiss National Science Foundation, the Institut Laue-Langevin, and the Swedish Natural Science Research Council are acknowledged for financial support. This work was also partially supported by the Swedish Superconductivity Consortium.

REFERENCES

1. J.-Y. Genoud, T. Graf, G. Triscone, A. Junod, and J. Muller, *Physica C* **192,** 137 (1992).
2. P. Bordet, C. Chaillout, J. Chenavas, J. L. Hodeau, M. Marezio, J. Karpinski, and E. Kaldis, *Nature* **334,** 596 (1988).
3. J. Karpinski, E. Kaldis, S. Rusiecki, E. Jilek, P. Fischer, P. Bordet, C. Chaillout, J. Chenavas, J. L. Hodeau, and M. Marezio, *J. Less-Common Met.* **150,** 129 (1989).
4. J. L. Tallon, D. M. Pooke, R. G. Buckley, M. R. Presland, and F. J. Blunt, *Phys. Rev. B* **41,** 7220 (1990).
5. J. Karpinski, E. Kaldis, S. Rusiecki, and E. Jilek, *J. Less-Common Met.* **164/165,** 3 (1990).
6. J.-Y. Genoud, T. Graf, A. Junod, G. Triscone, and J. Muller, *Physica C* **185–189,** 597 (1991).
7. P. Fischer, B. Roessli, J. Mesot, P. Allenspach, U. Staub, E. Kaldis, B. Bucher, J. Karpinski, S. Rusiecki, E. Jilek, and A. W. Hewat, *Physica B* **180/181,** 414 (1992).
8. H. Schwer, E. Kaldis, J. Karpinski, and C. Rossel, *Physica C* **211,** 165 (1993).
9. A. Matsushita, T. Yamanishi, Y. Yamada, N. Yamada, S. Takashima, S. Horii, K. Kawamoto, I. Hirabayashi, Y. Kodama, M. Otsuka, and T. Matsumoto, *Physica C* **227,** 254 (1994).
10. T. M. Chen, J. S. Ho, R. S. Liu, and H. S. Koo, *Physica C* **215,** 435 (1993).
11. D. B. Currie, M. T. Weller, P. C. Lanchester, and R. Walia, *Physica C* **224,** 43 (1994).
12. F. G. Tarntair and T. M. Chen, *Physica C* **235–240,** 367 (1994).
13. Y. Kodama, S. Tanemura, Y. Yamada, and U. Mizutani, *Physica C* **235–240,** 827 (1994).
14. N. Seiji, S. Adachi, and H. Yamauchi, *Physica C* **227,** 377 (1994).
15. R. G. Buckley, D. M. Pooke, J. L. Tallon, M. R. Presland, N. E. Flower, M. P. Staines, H. L. Johnson, M. Meylan, G. V. M. Williams, and M. Bowden, *Physica C* **174,** 383 (1991).
16. Y. X. Guo, R. Høier, T. Graf, and J.-Y. Genoud, *Phylosophical Mag. B* **72,** 383 (1995).
17. J. Karpinski, S. Rusiecki, B. Bucher, E. Kaldis, and E. Jilek, *Physica C* **161,** 618 (1989).
18. P. Berastegui, S.-G. Eriksson, L.-G. Johansson, M. Käll, L. Börjesson, M. Kakihana, and H. Mazaki, *Physica C* **259,** 97 (1996).
19. P. Berastegui, M. Kakihana, M. Yoshimura, H. Mazaki, H. Yasuoka, L.-G. Johansson, S. Eriksson, L. Börjesson, and M. Käll, *J. Appl. Phys.* **73,** 2424 (1993).
20. J. Rodriguez Carvajal, *Physica B* **192,** 55 (1993).
21. A. W. Hewat, P. Fisher, E. Kaldis, J. Karpinski, S. Rusiecki, and E. Jilek, *Physica C* **167,** 579 (1990).
22. J. Karpinski, S. Rusiecki, B. Bucher, E. Kaldis, and E. Jilek, *Physica C* **161,** 618 (1989).
23. R. J. Cava, A. W. Hewat, E. A. Hewat, B. Batlogg, M. Marezio, K. M. Rabe, J. J. Krajewski, W. F. Peck Jr., and L. W. Rupp Jr., *Physica C* **165,** 419 (1990).
24. G. Triscone, J.-Y. Genoud, T. Graf, A. Junod, and J. Muller, *Physica C* **201,** 1 (1992).
25. J. Karpinski, K. Conder, H. Schwer, Ch. Krüger, E. Kaldis, M. Maciejewski, C. Rossel, M. Mali, and D. Brinkmann, *Physica C* **227,** 68 (1994).
26. A. Kareiva, I. Bryntse, M. Karppinen, and L. Niinistö, *J. Solid State Chem.* **121,** 356 (1996).